Two-, three-, and four-photon ionization of Mg in the circularly and linearly polarized laser fields: Comparative study using the Hartree-Fock and model potentials

Gabriela Buica* and Takashi Nakajima†

Institute of Advanced Energy, Kyoto University,

Gokasho, Uji, Kyoto 611-0011, Japan

(Dated: February 11, 2013)

Abstract

We theoretically study multiphoton ionization of Mg in the circularly as well as the linearly polarized laser fields. Specifically two-, three-, and four-photon ionization cross sections from the ground and first excited states are calculated as a function of photon energy. Calculations are performed using the frozen-core Hartree-Fock and also the model potential approaches and the results are compared. We find that the model potential approach provide results as good as or even slightly better than those by the frozen-core Hartree-Fock approach. We also report the relative ratios of the ionization cross sections by the circularly and linearly polarized laser fields as a function of photon energy, which exhibit clear effects of electron correlations.

PACS numbers: 32.80.Rm

Keywords: Magnesium; Multiphoton ionization; Cross section; Hartree-Fock; Model potential

*Present address: Institute for Space Sciences, P.O. Box MG-23, Ro 77125, Bucharest-Măgurele, Romania

†E-mail address:t-nakajima@iae.kyoto-u.ac.jp (Takashi Nakajima)

I. INTRODUCTION

The interest for studying multiphoton ionization processes by using a circularly polarized (CP) field increased in the beginning of 1970's because of their potential of providing larger ionization cross sections in comparison to a linearly polarized (LP) field. Indeed, for a single-valence-electron atoms such as H and Cs, it has been shown in Refs. [1, 2] that the two- and three-photon ionization cross sections by the CP field are larger than those by the LP field. Soon after that, however, it was realized that this is not always true, especially for multiphoton resonant and near-resonant ionization processes in which more than a few photons are involved [3]. Depending on the atoms and the photon energy, cross sections by the LP field can be larger or smaller than those by the CP field. Reiss gave the correct interpretation of the CP and LP cross section ratio [3]: The ratio could be larger than one only for processes involving up to four- or five-photon ionization. This can be understood as a consequence of the following two reasons: First, if the number of photons involved for ionization is more than a few, there is more chance for the LP field than the CP field to be close to resonance with some bound states during multiphoton absorption. Second, since there are more ionization channels, in terms of the number of the accessible partial waves, for the LP field than the CP field, the sum of all these partial wave contributions could simply become larger for the LP field than the CP field. We note that most of the theoretical studies performed in the above context in those days is mainly for the single-valence-electron atoms and there are no published results for more complex atoms in a CP field.

Time has passed since then, and because of the significant development of theoretical methods and computer powers to calculate atomic structures, it is now possible to calculate multiphoton ionization cross sections for more complex atoms with reliable accuracy. Although there are quite a few theoretical reports for the multiphoton ionization cross sections beyond the single-valence-electron atoms such as Xe, He, Be, Mg, and Ca [4–13], all of them assumes the LP field. Although theoretical data for the multiphoton ionization cross sections for complex atoms by the CP field would provide complementary information to those by the LP field for the purpose of understanding the multiphoton dynamics, such data are still missing in the literature.

The purpose of this paper is to present theoretical results for the multiphoton ionization cross sections of Mg by the CP laser field by using the frozen-core Hartree-Fock (FCHF) and

model potential (MP) approaches. By comparing the calculated state energies and oscillator strengths, we find that the MP approach is as good as the FCHF approach for the oscillator strengths. As for the state energies, the MP approach gives even better numbers than the FCHF approach. As a result, for the purpose of calculating multiphoton ionization cross sections of Mg, the MP approach could give even slightly better numbers than the FCHF approach. As additional data, we also provide the *ratios* of the multiphoton ionization cross sections by the LP and CP fields, which would be very useful from the experimental point of view, since the *absolute* measurement of the multiphoton ionization cross sections is usually very difficult. The ratio of the multiphoton ionization cross sections of Mg by the CP and LP fields we have obtained exhibits a similar behavior with those reported for the single-valence-electron atoms as well as rare gas atoms [1, 2, 14, 15].

II. THEORETICAL APPROACH

The Mg atom is a *two-valence-electron* atom; it consists of a closed core (the nucleus and the 10 inner-shell electrons) and two-valence electrons. As it is already mentioned in the literature [16] there are several approaches to solve the Schrödinger equation for one- and two-valence-electron atom in a laser field. Since the general computational procedure has already been presented in Refs. [6, 9, 10] and the specific details about the atomic structure calculation of Mg have been reported in recent works [11, 12], we only briefly describe the method we employ. The field-free one-electron Hamiltonian of Mg^+, $H_a(r)$, is expressed, in a.u., as:

$$H_a(r) = -\frac{1}{2}\frac{\mathrm{d}^2}{\mathrm{d}r^2} - \frac{Z}{r} + \frac{l(l+1)}{2r^2} + V_{eff}(r), \tag{1}$$

where $V_{eff}(r)$ is the effective potential acting on the valence electron of Mg^+. r represents the position vector of the valence electron, Z the core charge (= 2 in our case), and l the angular quantum number. Depending on how we describe $V_{eff}(r)$, we consider two approaches in this paper, the FCHF and the MP methods.

A. One-Electron Orbitals: Frozen-Core Hartree-Fock approach

The most widely used approach to describe the ionic core would be the FCHF approach. In the FCHF approach the ionic core of Mg^{2+} ($1s^2 2s^2 2p^6$) is given by:

$$V_{eff}(r) = V_l^{HF}(r) + V_l^p(r), \tag{2}$$

where V_l^{HF} represents the FCHF potential (FCHFP) and V_l^p is the core-polarization potential which effectively accounts for the interaction between the closed core and the valence electrons [6]. Specifically we employ the following form for the core-polarization. $V_l^p(r) = -\frac{\alpha_s}{2r^4}\left[1 - \exp^{-(r/r_l)^6}\right]$, in which α_s is the static dipole polarizability of Mg^{2+} and r_l the cut-off radii for the different orbital angular momenta, $l = 0, 1, 2, ...$, etc. For the expansion of one-electron orbitals, we employ a B-spline basis set. Thus, solving the Schrödinger equation for the nonrelativistic Hamiltonian defined in Eq. (1) with the FCHFP is now equivalent to the eigenvalue problem.

B. One-Electron Orbitals: Model potential approach

Another simpler way to describe the ionic core is to use a MP, V_l^{MP} [17–20] instead of the FCHFP, V_l^{HF}. The advantage of the MP approach is that, we practically solve the Schrödinger equation for the two-valence electrons outside the frozen-core which is now modeled by the pseudopotential, and thus the complexity of the problem is greatly reduced. To start with, we employ the pseudopotential reported in [21] to describe the ionic core of Mg:

$$V_l^{MP}(r) = -\frac{A}{r}\exp\left(-\alpha r^2\right) + B_l \exp\left(-\beta_l r^2\right), \tag{3}$$

where $A = 0.583, \alpha = 0.439, B_0 = 11.101, \beta_0 = 1.383, B_1 = 5.220, \beta_1 = 0.995, B_{l\geq 2} = 0$, and $\beta_{l\geq 2} = 0$ [21]. Note that the core-polarization potential, V_l^p, is not included in Eq. (3).

In addition to the MP shown in Eq. (3) (named MP^a), we have obtained a new model potential with a core-polarization term, V_l^p, named MP^b, in the following way: We have added the core-polarization term to Eq. (3) and performed least-squares fittings for A and α with α_s fixed to 0.491 [22], to the lowest three states of d and f series of Mg^+ simultaneously. Having fitted A and α, we proceed to perform fittings for B_0 and β_0, and B_1 and β_1, respectively, to the lowest three states of s and p series of Mg^+. After these

procedures, the fitted MP^b parameters with the core-polarization term are, $A = 0.541, \alpha = 0.561, B_0 = 11.086, \beta_0 = 1.387, B_1 = 5.206, \beta_1 = 1.002, B_{l\geq 2} = 0$, and $\beta_{l\geq 2} = 0$ together with the cut-off radii $r_0 = 1.241$, $r_1 = 1.383$, $r_2 = 1.250$, $r_3 = 1.300$, and $r_4 = 1.100$. We note that this form of V_l^{MP} is different from the one used in Refs. [18, 19] (named MP^c). In Section III, we will make comparisons for the results obtained by FCHFP, MP^a, MP^b, and MP^c.

C. Two-Electron States and Ionization Cross Section

Once the one-electron orbitals have been obtained using either FCHFP or MP, we can construct two-electron states as we describe below: The field-free two-electron Hamiltonian, $H_a(\mathbf{r}_1, \mathbf{r}_2)$, can be expressed, in a.u., as,

$$H_a(\mathbf{r}_1, \mathbf{r}_2) = \sum_{i=1}^{2} H_a(r_i) + V(\mathbf{r}_1, \mathbf{r}_2), \tag{4}$$

where $H_a(r_i)$ represents the one-electron Hamiltonian for the i^{th} electron as shown in Eq. (1), and $V(\mathbf{r}_1, \mathbf{r}_2)$ is a two-body interaction operator, which comprises the static Coulomb interaction $1/|\mathbf{r}_1 - \mathbf{r}_2|$ and the dielectronic effective interaction [6, 22]. $\mathbf{r}_1$ and $\mathbf{r}_2$ are the position vectors of the two valence electrons. By solving the two-electron Schrödinger equation for the Hamiltonian given in Eq. (4), two-electron states are constructed with the configuration interaction approach [6, 9, 10]. Since Mg is a light atom and the LS-coupling description is known to be good, it is sufficient to label the states by L, S, J, and M_J which represent the total orbital angular momentum, total spin angular momentum, total angular momentum, and its projection onto the quantization axis, respectively. Furthermore, if we assume that the initial state is a singlet state ($S = M_S = 0$), J and M_J, respectively, become identical with L and M_L. Thus, the singlet states can be labeled by L and M_L only.

Once the two-electron wave functions have been obtained, the two-electron dipole matrix elements can be calculated from state $|LM_L\rangle$ to state $|L'M'_L\rangle$ for both LP and CP fields. Specifically we calculate the effective N-photon bound-free transition amplitude from the ground state of Mg, i.e., $3s^2\ ^1S^e$ ($L = 0, M_L = 0, S = 0, M_S = 0$). The singlet-triplet transitions for the Mg atom are extremely weak and we can safely neglect them. Owing to the dipole selection rules for the magnetic quantum number, namely $\Delta M_L = +1$ for the RCP field and $\Delta M_L = 0$ for the LP field, starting from the ground

state with $L = M_L = 0$, the allowed dipole transitions by the single-photon absorption are $|L,\ M_L = L\rangle \rightarrow |L' = L+1,\ M'_L = L+1\rangle$ for the CP field in comparison to $|L,\ M_L = 0\rangle \rightarrow |L' = L+1,\ M'_L = 0\rangle$ for the LP field.

Having obtained the individual two-electron dipole matrix elements we can calculate the effective N-photon bound-free transition amplitude from the initial bound state, $|i\rangle$, to the final continuum state, $|f\rangle$, within the lowest-order perturbation theory (LOPT). In atomic units, it reads,

$$\begin{aligned} \mathcal{M}_{if}^{(N)}(\omega) = & \sum_{m_1} ... \sum_{m_{N-1}} \frac{\langle f|D_q|m_{N-1}\rangle \langle m_{N-1}|D_q|m_{N-2}\rangle}{E_{m_{N-1}} - E_i - (N-1)\omega} \\ & ... \times \frac{\langle m_2|D_q|m_1\rangle \langle m_1|D_q|i\rangle}{E_{m_1} - E_i - \omega}, \end{aligned} \tag{5}$$

where D_q denotes the spherical component of the dipole operator with $q = 0, \pm 1$ for the LP, RCP, and left-CP (LCP) fields, respectively. E_f, E_g, and E_{m_k} are the state energies, and ω represents the photon energy. Summation is taken over all possible (both bound and continuum) intermediate states, $\{|m_k\rangle\}$ $(k = 1, 2, ..., N-1)$. Note that Eq. (5) is valid for both length and velocity gauge. In the length gauge the dipole operator is expressed as $D = -\mathbf{E}(t) \cdot (\mathbf{r}_1 + \mathbf{r}_2)$, and $D = -\mathbf{A}(t) \cdot (\mathbf{p}_1 + \mathbf{p}_2)$ in the velocity gauge, respectively. $\mathbf{A}(t)$ is the vector potential of the electric field vector $\mathbf{E}$ (t). From Eq. (5) it should be clear that the differences of the N-photon bound-free transition amplitudes by the LP and CP fields come from the angular coefficient which is implicit in the individual dipole matrix elements for different q, i.e., $\langle m_{k+1}|D_q|m_k\rangle$, and the accessible intermediate as well as the final states due to the dipole selection rules as we have illustrated above. Finally, the generalized N-photon partial ionization cross section from the ground state, $|g\rangle$, to the continuum state, $|c_L\rangle$, is given in a.u., within LOPT, by [4],

$$\sigma_{gc_L}^{(N)}(\omega) = 2\pi(2\pi\alpha)^N \omega^N \left|\mathcal{M}_{gc_L}^{(N)}(\omega)\right|^2 , \tag{6}$$

where α represents the fine structure constant.

III. NUMERICAL RESULTS AND DISCUSSION

Now we present numerical results for the total and partial two-, three-, and four-photon ionization cross sections from the ground state of Mg by the LP and RCP fields. For the calculation of the individual dipole matrix elements in Eq. (5), a spherical box of radius

$\sim$ 300 a.u. and a number of 302 B-spline polynomials of order 9 and the total angular momenta from $L = 0$ up to $L = 4$ are employed to represent one-electron orbitals. In order to resolve the sharp resonance peaks appearing in the ionization cross sections graphs, the box radius is varied from 300 to 320 a.u. with a step of 1 a.u.. We have confirmed that the calculated cross sections in both length and velocity gauge are in very good agreement for the FCHFP approach. As for the MP approach, however, it is well known that the correct dipole matrix elements are given only in the length gauge [23], since the Hamiltonian becomes nonlocal due to the l-dependent model potential (see Eq. (3)). In other words the disagreement, if any, between the results in the length and velocity gauge for the MP approach with l-dependent model potentials does not imply the doubt on the reliability of the calculated results, but rather it is a measure of the nonlocality of the l-dependent model potential. The same argument holds for the pseudopotential. Therefore all the results for the MP approach reported in this paper have been calculated in the length gauge only.

In Table I we show the comparison of calculated energies by the FCHFP, MP^a, MP^b, and MP^c [19], and the experimental data for the ionization threshold and the two-electron states for the first few low-lying states. All energies have been taken with respect to the energy of Mg^{2+} and the experimental data have been taken from the database of National Institute of Standards and Technology (NIST). From Table I we notice that the MP^a, MP^b, and MP^c provide more accurate energies than the FCHFP for the ionization threshold and the first few low-lying states. In particular the ground state energy is better described by the MP^a and MP^b. Of course, accuracy of the calculated energies does not always guarantee the accuracy of the wavefunction, and we now check the accuracy of the wavefunction in terms of the oscillator strengths. Table II presents comparisons of the oscillator strengths for a single-photon absorption in Mg calculated by the FCHFP, MP^a, MP^b, and MP^c, and the experimental data. The calculated values are shown for the following single-photon transitions: $3s^2\ ^1S^e \rightarrow 3s(3-6)p\ ^1P^o$, $3s3p\ ^1P^o \rightarrow 3s(4-7)s\ ^1S^e$, $3s3p\ ^1P^o \rightarrow 3s(3-6)d\ ^1D^e$, $3s3d\ ^1D^e \rightarrow 3s(4-7)p\ ^1P^e$, and $3s3d\ ^1D^e \rightarrow 3s(4-7)f\ ^1F^o$. At first glance we see that both FCHFP and MP^b give accurate values which are comparable with the experimental data but relatively large differences appear for the MP^a, especially in case of the $3s^2 \rightarrow 3s(5-6)p$, $3s3p \rightarrow 3s5s$, $3s3d \rightarrow 3s(5-7)p$ transitions where the differences can reach 30% for the $3s3d \rightarrow 3s5p$ and $3s7p$ transitions. As one can easily understand, these results indicate that the inaccuracy of the MP^a most likely comes from the neglect of core-polarization.

Similarly, for the MP^c some small differences appear in the oscillator strengths for the $3s3p \rightarrow 3s(3-6)d$ and $3s3d \rightarrow 3s(5-6)p$ transitions. From the comparisons presented in Tables I and II, it is clear that, although both MP^a and MP^b provide more accurate values for the state energies than FCHFP, the MP^b and FCHFP provide better accuracy for the oscillator strengths. Therefore, in what follows we present results of multiphoton ionization cross sections obtained by the FCHFP and MP^b only.

First we present numerical results for the two-, three-, and four-photon ionization cross sections from the ground state of Mg by the LP and RCP fields by using the FCHFP. Figure 1(a) shows the partial two-photon ionization cross sections by the LP field, leading to the $^1S^e$ (dashed) and $^1D^e$ continua (solid) as a function of photon energy, which are in good agreement with those in the literature [10–12]. As for two-photon ionization by the CP field there is only one ionization channel, and the ionization cross section to the $^1D^e$ continuum is shown in Fig. 1(b). The solid line in Fig. 1(c) presents the ratio of the two-photon ionization cross sections by the CP and LP fields, $\sigma^{(2)}_{CP}/\sigma^{(2)}_{LP}$, as a function of photon energy. For a wide range of photon energy two-photon ionization by the CP field turns out to be more efficient unless there is near-resonant state(s). The ratio of the two-photon ionization cross sections is in very good agreement with the results presented in Refs. [8, 12]. Furthermore the maximum value of the ratio is very close to the ones reported for the single-valence-electron atoms [1, 2, 14, 24] and rare gas atoms [15], namely ~ 1.5. Although the reason why we obtain similar values seems to be simply connected to the geometric effects (i.e., angular coefficients) starting from the S symmetry, as employed in the calculation of the dipole matrix elements for the single-valence-electron atoms [25], it turned out that the things are not so simple, as we will show later on in this paper.

Next we calculate the partial three-photon ionization cross sections leading to the $^1P^o$ (dashed) and $^1F^o$ (solid) continua. The result is shown in Fig. 2(a) for the LP field. Again our result is in good agreement with those in the literature [10, 12]. The three-photon ionization cross section by the CP field is shown in Fig. 2(b) where the accessible continuum is $^1F^o$ only. The solid line in Fig. 2(c) presents the ratio of the three-photon ionization cross sections by the CP and LP fields, $\sigma^{(3)}_{CP}/\sigma^{(3)}_{LP}$, as a function of photon energy. Again, as in the case of two-photon ionization the maximum value of the ratio is very close to the one reported for the single-valence-electron atoms and rare gas atom [1, 2, 14, 15], namely ~ 2.5.

Figure 3(a) shows the partial four-photon ionization cross sections leading to the $^1S^e$

(dot-dashed), $^1D^e$ (dashed), and $^1G^e$ continua (solid) as a function of photon energy for the LP field, which is in good agreement with those in Refs. [11, 12]. Since there are three ionization channels for the LP field in contrast to only one ionization channel for the CP field, we expect that ionization by the LP field starts to be more efficient than that by the CP field. For the CP field the four-photon ionization cross section into the ^1G continuum is plotted in Fig. 3(b), and the ratio of the cross sections by the CP and LP fields, $\sigma^{(4)}_{CP}/\sigma^{(4)}_{LP}$, is shown by the solid line in Fig. 3(c). The maximum value of the ratio is ~ 4.4 while the minimum value is almost zero. Figure 3(c) indicates that four-photon ionization by the LP field starts to become more efficient than that by the CP field around the photon energy of $1.9 - 2.1$ and $2.2 - 2.3$ eV. Indeed, because of the multiphoton-character of the ionization process and the dense energy levels of the Mg atom, more and more intermediate states become close to resonance by the LP field compared with the CP field, thus, contributing to the ionization efficiency.

The Mg atom is known to have strong electron correlations, and their effect on the multiphoton ionization spectra and oscillator strengths has been reported in, for example, Refs. [10, 26]. For atoms with strong electron correlations, the values of oscillator strengths and ionization cross sections themselves naturally deviate from the accurate ones if the electron correlation is not fully taken into account. Now we examine the effect of electron correlation in a different context: The question we address now is whether the *ratios* of the multiphoton ionization cross sections by the LP and CP fields significantly differ with/without electron correlations taken into account. Naively we expect that the change of the ratios would be less sensitive to that of the cross sections themselves. To investigate this, we have repeated the calculations for two simplified configurations: (I) with a form of $3snl$ ($n = 3, 4, ...$) only, and (II) $3snl$, $3p^2\ ^1P^o$, $3p(3-5)d\ ^1D^e$, and $3p(4-6)s\ ^1P^o$. The results for the configurations (I) and (II) are shown by the dashed and dot-dashed lines in Figs. 1(c), 2(c), and 3(c) for two-, three-, and four-photon ionization, respectively, with remarkable differences. For the convenience of comparison, the ground state energy for the simplified configuration (I) has been shifted to the accurate values since the energy deviation turned out to be large. Recalling that the multiphoton ionization spectra are known to be mostly dominated by the resonant structures arising from the intermediate singly excited bound states [10], we attribute these differences mainly to the modification of the bound state wave functions, although the differences we see for two-photon ionization (Fig. 1(c)) indicate the modifica-

tion of the continuum states as well as the bound states due to the presence of the doubly excited states $3p^2$ and $3p4p$. From these comparisons it is clear that, although the maximal value of the ratios of Mg turned out to be similar to those for single-valence-electron atoms, the physical origin of the similarity would not be the geometric effects, since, if so, the ratios calculated by the simplified configurations (I) should not so much differ from others: The angular coefficients are the same for both full and simplified configurations. Based on this argument, we conclude that the differences in the ratios for the different configurations are essentially due to the dynamic effect (electron correlation) rather than the geometric effect.

The results presented in Figs. 1-3 are multiphoton ionization cross sections from the ground states. Now, in Figs. 4(a) and (b), we present, for the first time, the two- and three-photon ionization cross sections from the first excited state $3s3p\ ^1P^o$ of Mg by the CP laser field. The two-photon ionization cross section from $3s3p\ ^1P^o$ is dominated by the single-photon resonances with the $3snd\ ^1D^e$ $(n = 4, 5, ...)$ bound excited states while the three-photon ionization cross section is dominated by the single-photon resonance due to the $3s3d\ ^1D^e$ state and two-photon resonances with the $3snf\ ^1F^o$ $(n = 4, 5, ...)$ bound excited states.

Finally, we present comparisons for the *total* two-, three-, and four-photon ionization cross sections from the ground state of Mg by the LP and RCP fields by using the FCHFP and MP^b. Comparison of the total two-photon ionization cross sections by the LP and RCP fields using the FCHFP (solid) and MP^b (dot-dashed) are plotted in Figs. 5 (a) and (b), respectively. Apart from the slight energy shift, we find that the agreement is very good. At the photon energy $\omega = 4.65$ eV corresponding to the third harmonic of a Ti-sapphire laser, the total two-photon ionization cross sections by the LP field are 7.2 $\times 10^{-48}$ cm^4 s and 8.89 $\times 10^{-48}$ cm^4 s calculated by the FCHFP and MP^b, respectively. Similarly, the total three- and four-photon ionization cross sections by the LP and RCP fields using the FCHFP (solid) and MP^b (dot-dashed) are compared in Figs. 6 and 7(a)-(b), respectively. The small energy shift which is present in all three cross section graphs Figs. 5-7 is mainly due to the better description of the ground state energy by the MP^b than the FCHFP (see Table I). The total three-photon ionization cross sections by the LP field at the photon energy $\omega = 3.1$ eV corresponding to the second harmonic of a Ti-sapphire laser are 1.0 $\times 10^{-80}$ cm^6 s^2 and 1.05 $\times 10^{-80}$ cm^6 s^2 calculated by the FCHFP and MP^b, respectively. At $\omega = 2.33$ eV, Tang *et al.* [9] reported a value of 1.66 $\times 10^{-113}$ cm^6 s^2 which agrees to ours of 1.86 $\times 10^{-113}$ cm^6 s^2

and 1.69 $\times 10^{-113}$ cm^6 s^2 by the FCHFP and MP^b, respectively. From these comparisons of the multiphoton ionization cross sections presented in Figs. 5-7 and those in the literature [9] we consider that the model potential (MP^b) we report in this paper works quite well to describe the Mg atom compared with the FCHFP with a core-polarization correction.

IV. CONCLUSIONS

In conclusion, based on the ab-initio method, we have reported the two-, three-, and four-photon ionization cross sections from the ground and first excited states of Mg by the CP field using the frozen-core Hartree-Fock method and compared the results with those obtained by the model potential method with a core-polarization correction. We have found that the use of the appropriate model potential can lead to comparable or even slightly better description for multiphoton ionization of Mg.

From the extensive calculations, we have found that depending on the photon energy the two- and three-photon ionization cross sections are generally larger for the CP field than the LP field, while starting with four-photon ionization the result might be reversed, which qualitatively agrees with the results for the single-valence-electron atoms and rare gas atoms [1, 2, 14, 15]. This similarity has been clearly seen in the variation of the ratios of multiphoton ionization cross sections rations by the CP and LP fields. The physical origin of the similarity, however, turned out to be different: For our case at hand, it is the dynamic (electron correlation) effects rather than the geometric effects, that determines the ratios, while for the cases in Refs. [1, 2, 14, 15] the dominant contribution would be the geometric effects.

Related to the above, we have also studied the influence of electron correlation in terms of the change of the *ratios* of multiphoton ionization cross sections by the CP and LP fields, which we primarily assumed to be less sensitive than the values of the cross sections themselves, since some effects of electron correlation can be canceled out when the ratios are taken. Careful examinations have revealed, however, that the clear effects of electron correlation are seen in not only the cross sections but also in their ratios.

Acknowledgments

G.B. acknowledges financial support from Japan Society for the Promotion of Science. The work by T.N. was supported by a Grant-in-Aid for scientific research from the Ministry of Education and Science of Japan.

---

[1] Gontier Y, Trahin M. Multiphoton Ionization Induced by Circularly Polarized Radiation. Phys Rev A 1973;7:2069-2073; Multiphoton Processes in a Hydrogen Atom. Phys Rev A 1971;4:1896-1906.

[2] Lambropoulos P. Effect of Light Polarization on Multiphoton Ionization of Atoms. Phys Rev Lett 1972;28:585-587.

[3] Reiss HR. Polarization Effects in High-Order Multiphoton Ionization. Phys Rev Lett 1972;29:1129-1131.

[4] L'Huillier A, Tang X, Lambropoulos P. Multiphoton ionization of rare gases using multichannel-quantum-defect theory. Phys Rev A 1989;39:1112-1122.

[5] Saenz A, Lambropoulos P. Theoretical two-, three- and four-photon ionization cross sections of helium in the XUV range. J Phys B 1999;32:5629-5637.

[6] Chang TN. Many-body theory of Atomic Structure and Photoionization. Singapore:World Scientific, 1993. p 213-247.

[7] Tang X, Bachau H. Three-photon ionization cross section calculations of Be. J Phys B 1993;26:75-83.

[8] Moccia R, Spizzo P. Atomic magnesium: II. One-photon transition probabilities and ionization cross sections. A valence-shell L^2 CI calculation. J Phys B 1988;21:1133-1143; Atomic magnesium: III. Two-photon transition probabilities and ionization cross sections: A valence-shell L^2 CI calculation. J Phys B 1988;21:1145-1154.

[9] Tang X, Chang TN, Lambropoulos P, Fournier S, and DiMauro L. Multiphoton ionization of magnesium with configuration-interaction calculations. Phys Rev A 1990;41:5265-5268.

[10] Chang TN, Tang X. Atomic-structure effects in multiphoton ionization of magnesium. Phys Rev A 1992;46:R2209-R2212.

[11] Buica-Zloh G, and Nikolopoulos LAA. Multiphoton ionization of magnesium in a Ti-sapphire

laser field. Eur Phys J D 2004;29:245-251.

[12] Nikolopoulos LAA. Mg in electromagnetic fields: Theoretical partial multiphoton cross sections. Phys Rev A 2005;71:033409-1-033409-8.

[13] Benec'h S, Bachau H. One-, two- and three-photon ionization of calcium. J Phys B 2004;37:3521-3534.

[14] McGuire EJ. Green's-function approach to nonresonance multiphoton absorption in the alkali-metal atoms. Phys Rev A 1981;23:186-200.

[15] McGuire EJ. Two- and three-photon ionization in the noble gases. Phys Rev A 1981;24:835-848.

[16] Bachau H, Cormier E, Decleva P, Hansen JE, Martin F. Applications of B-splines in atomic and molecular physics. Rep Prog Phys 2001;64:1601-1943.

[17] Mengali S, Moccia R. Non-empirical core-polarization effects on the optical properties of Mg(I): II. Bound-bound and bound-free one- and two-photon transitions up to the third ionization threshold. J Phys B 1996;29:1613-1628.

[18] Aymar M, Greene CH, Luc-Koenig E. Multichannel Rydberg spectroscopy of complex atoms. Rev Mod Phys 1996;68:1015-1123.

[19] Luc-Koenig E, Lyras A, Lecomte J-M, Aymar M. Eigenchannel R-matrix study of two-photon processes including above-threshold ionization in magnesium. J Phys B 1997;30:5213-5232.

[20] Moccia R, Spizzo P. Atomic magnesium: Discrete and continuum spectrum properties from a valence-shell L^2 configuration-interaction calculation with polarization potential. Phys Rev A 1989;39:3855-3860.

[21] Preuss H, Stoll H, Wedig U, Krüger T. Combination of pseudopotentials and density functionals. Int J Quant Chem 1981;19:113-130.

[22] Mengali S, Moccia R. Non-empirical core polarization effects on the optical properties of Mg(I): I. Discrete and continuum energy spectrum up to the third ionization threshold . J Phys B 1996;29:1597-1611.

[23] Starace A. Length and velocity formulas in approximate oscillator strength calculation. Phys Rev A 1971;3:1242-1245; Kobe D H. Gauge-invariant resolution of the controversy over length versus velocity forms of the interaction with electric dipole radiation. Phys Rev A 1979;19:205-214.

[24] Teague MR, Lambropoulos P, Goodmanson D, Norcross DW. Theory of two-photon ionization

of cesium. Phys Rev A 1976;14:1057-1064.

[25] Klarsfeld S, Maquet A. Circular versus Linear Polarization in Multiphoton Ionization. Phys Rev Lett 1972;29:79-81.

[26] Chang TN. Effect of the configuration interaction on the theoretical oscillator strengths of the magnesium atom. Phys Rev A 1987;36:447-455.

Table I. Comparison of the energies for the ionization threshold and the few bound states states of Mg. The energies are expressed in eV with respect to the energy of Mg^{2+}.

	FCHFP	MP[a]	MP[b]	MP[c]	Exp
E_{Mg^+}	−14.999555	−15.035553	−15.049135	−15.035241	−15.035266
E_{3s3s}	−22.577	−22.748	−22.666	−22.585	−22.681497
E_{3s4s}	−17.236	−17.301	−17.288	−17.264	−17.2877715
E_{3s5s}	−16.123	−16.170	−16.169	−16.157	−16.1653583
E_{3s6s}	−15.677	−15.717	−15.721	−15.711	−15.715213
E_{3s3p}	−18.277	−18.313	−18.327	−18.302	−18.3356944
E_{3s4p}	−16.521	−16.559	−16.566	−16.553	−16.5632827
E_{3s5p}	−15.860	−15.898	−15.904	−15.894	−15.8987514
E_{3s6p}	−15.551	−15.588	−15.594	−15.586	−15.5877425
E_{3s3d}	−16.888	−16.966	−16.936	−16.905	−16.9282505
E_{3s4d}	−16.056	−16.110	−16.101	−16.082	−16.0936414
E_{3s5d}	−15.663	−15.707	−15.707	−15.694	−15.700148
E_{3s6d}	−15.451	−15.491	−15.494	−15.484	−15.4875318
E_{3s4f}	−15.867	−15.903	−15.909	−15.902	−15.9024831
E_{3s5f}	−15.553	−15.590	−15.596	−15.589	−15.5890852
E_{3s6f}	−15.383	−15.419	−15.426	−15.419	−15.4190639
E_{3s7f}	−15.281	−15.317	−15.323	−15.317	−15.3167415

Table II. Comparison of the absorption oscillator strengths (in atomic units) between states with $^1S^e$, $^1P^o$, and $^1D^e$ symmetry.

$3s^2\ ^1S^e \rightarrow$	$3s3p\ ^1P^o$	$3s4p\ ^1P^o$	$3s5p\ ^1P^o$	$3s6p\ ^1P^o$
FCHFP	1.7659	0.1142	2.518(−2)	9.297(−3)
MP[a]	1.7519	0.1217	2.745(−2)	1.023(−2)
MP[b]	1.7677	0.1162	2.588(−2)	9.606(−3)
MP[c]	1.7619	0.1145	2.535(−2)	9.371(−3)
Exp	1.8	0.113	2.4(−2)	9.1(−3)
$3s3p\ ^1P^o \rightarrow$	$3s4s\ ^1S^e$	$3s5s\ ^1S^e$	$3s6s\ ^1S^e$	$3s7s\ ^1S^e$
FCHFP	0.1547	6.433(−3)	1.517(−3)	5.570(−4)
MP[a]	0.1553	5.901(−3)	1.403(−3)	5.255(−4)
MP[b]	0.1543	6.288(−3)	1.481(−3)	5.447(−4)
MP[c]	0.1552	6.453(−3)	1.510(−3)	5.493(−4)
Exp	0.155	6.3(−3)	1.5(−3)	
$3s3p\ ^1P^o \rightarrow$	$3s3d\ ^1D^e$	$3s4d\ ^1D^e$	$3s5d\ ^1D^e$	$3s6d\ ^1D^e$
FCHFP	0.244	0.1076	0.1188	8.666(−2)
MP[a]	0.218	0.1346	0.1282	8.814(−2)
MP[b]	0.240	0.1025	0.1196	8.659(−2)
MP[c]	0.262	9.299(−2)	0.1010	8.255(−2)
Exp	0.245	0.106	0.121 ± 0.01	8.7(−2)
$3s3d\ ^1D^e \rightarrow$	$3s4p\ ^1P^o$	$3s5p\ ^1P^o$	$3s6p\ ^1P^o$	$3s7p\ ^1P^o$
FCHFP	0.1357	5.886(−3)	2.223(−3)	1.165(−3)
MP[a]	0.1351	7.494(−3)	2.835(−3)	1.479(−3)
MP[b]	0.1352	5.963(−3)	2.253(−3)	1.180(−3)
MP[c]	0.1361	5.314(−3)	2.005(−3)	1.053(−3)
Exp	0.146	5.92(−3)	2.3(−3)	1.1(−3)
$3s3d\ ^1D^e \rightarrow$	$3s4f\ ^1F^o$	$3s5f\ ^1F^o$	$3s6f\ ^1F^o$	$3s7f\ ^1F^o$
FCHFP	0.5150	0.1437	6.218(−2)	3.321(−2)
MP[a]	0.4742	0.1387	6.117(−2)	3.3(−2)
MP[b]	0.5082	0.1430	6.204(−2)	3.319(−2)
MP[c]	0.5336	0.1460	6.263(−2)	3.33(−2)
Exp	0.514	0.143	6.2(−2)	3.3(−2)

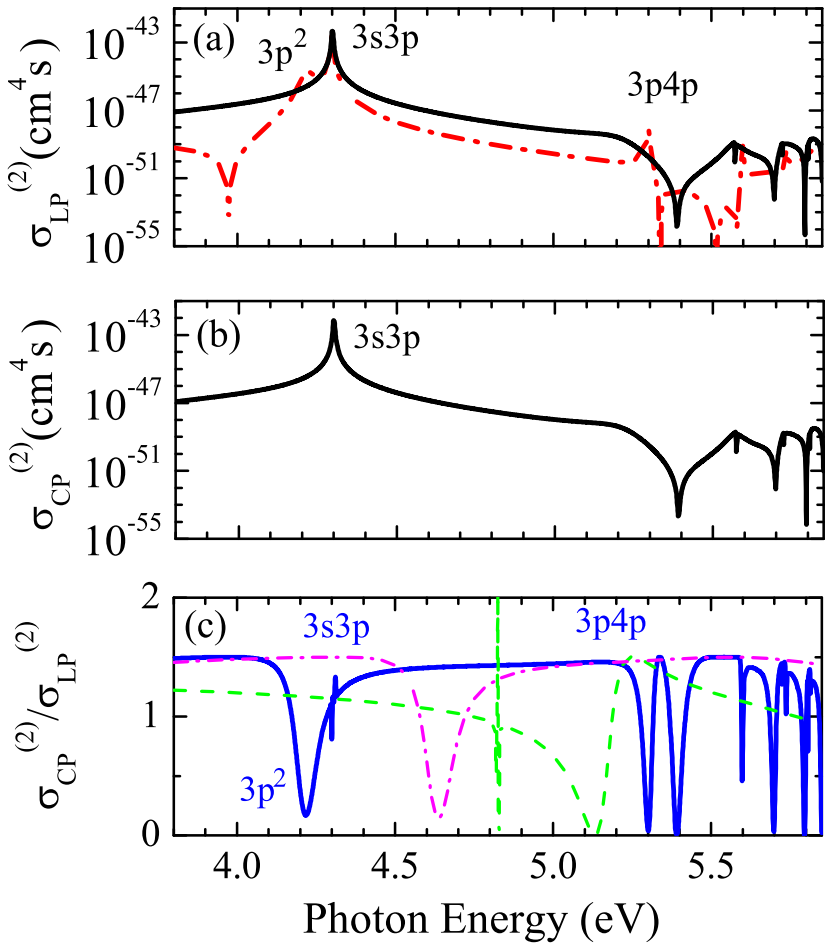

FIG. 1: (Color Online) (a) Partial two-photon ionization cross sections, $\sigma^{(2)}_{LP}$, by the LP field, leading to the ^1S (dashed) and ^1D (solid) continua, as a function of photon energy. (b) Two-photon ionization cross section, $\sigma^{(2)}_{CP}$, by the CP field. (c) Ratio of the two-photon ionization cross sections by the CP and LP fields, $\sigma^{(2)}_{CP}/\sigma^{(2)}_{LP}$, as a function of photon energy. Results for the full configuration, and simplified configurations (I) and (II) are shown by the solid, dashed, and dot-dashed lines, respectively.

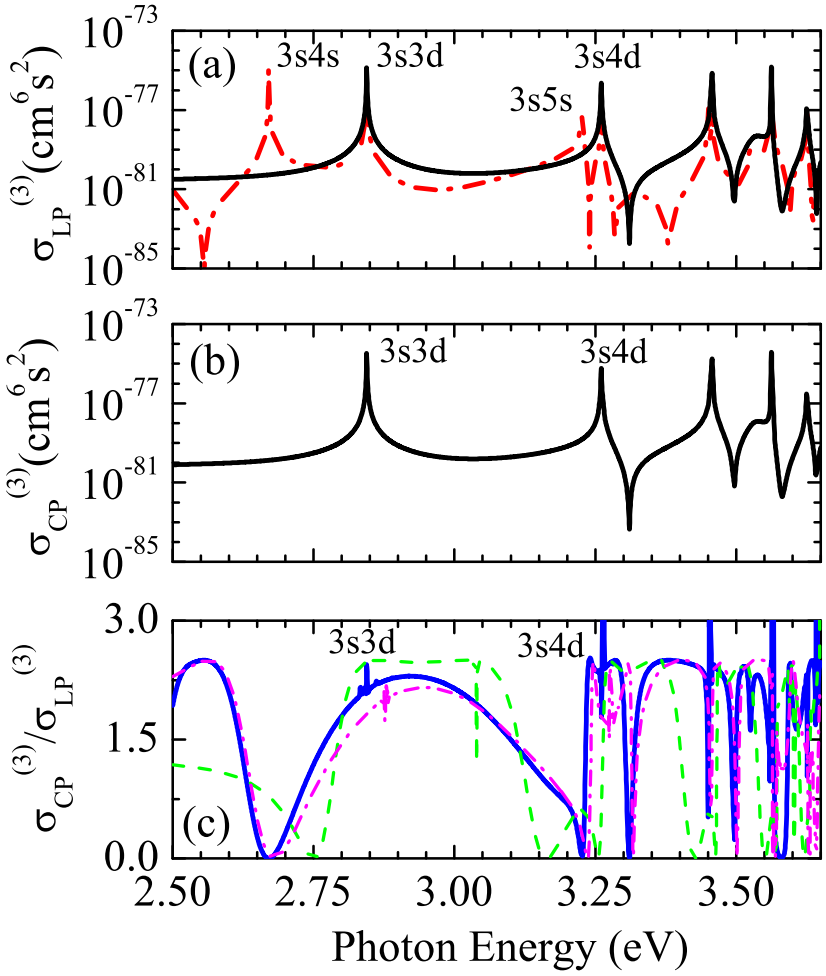

FIG. 2: (Color Online)(a) Partial three-photon ionization cross sections, $\sigma^{(3)}_{LP}$, by LP the field, leading to the ^1P (dashed) and ^1F (solid) continua, as a function of photon energy. (b) Three-photon ionization cross section $\sigma^{(3)}_{CP}$ by the CP field. (c) Ratio of the three-photon ionization cross sections by the CP and LP fields, $\sigma^{(3)}_{CP}/\sigma^{(3)}_{LP}$, as a function of photon energy. Results for the full configuration, and simplified configurations (I) and (II) are shown by the solid, dashed, and dot-dashed lines, respectively.

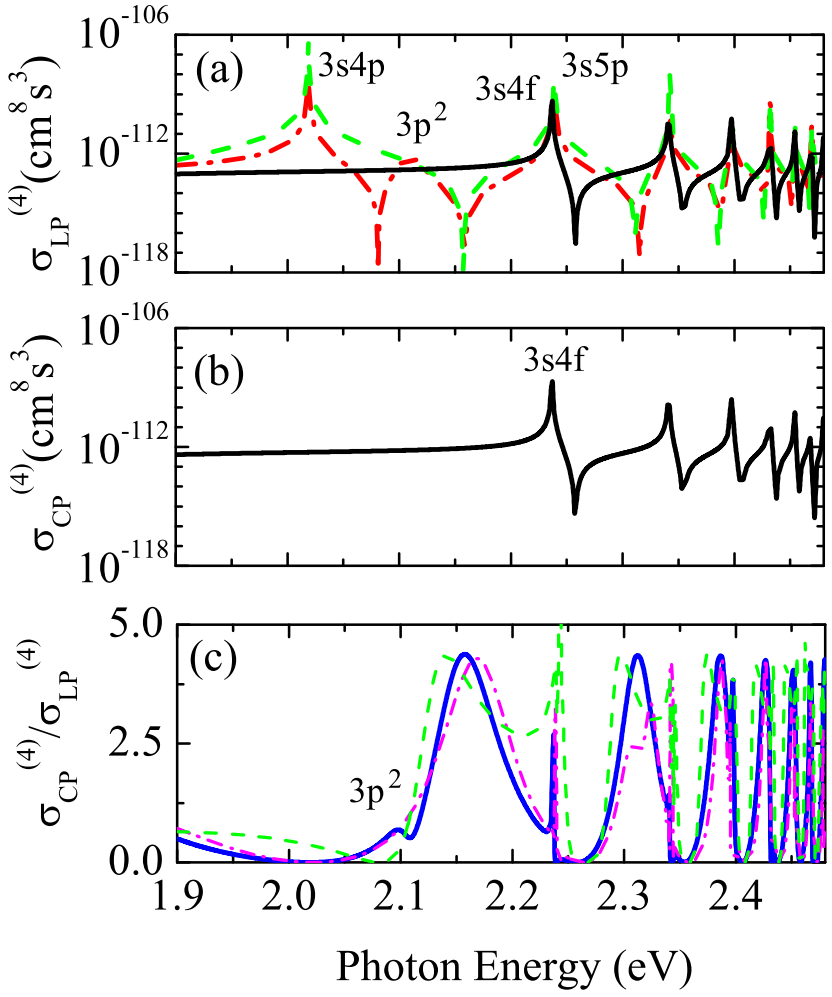

FIG. 3: (Color Online) (a) Partial four-photon ionization cross sections, $\sigma^{(4)}_{LP}$, by the LP field, leading to the ^1S (dot-dashed), ^1D (dashed) and ^1G (solid) continua, as a function of photon energy. (b) Four-photon ionization cross section, $\sigma^{(4)}_{CP}$, by the CP field. (c) Same as that in Fig. 1(c) but for four-photon ionization.

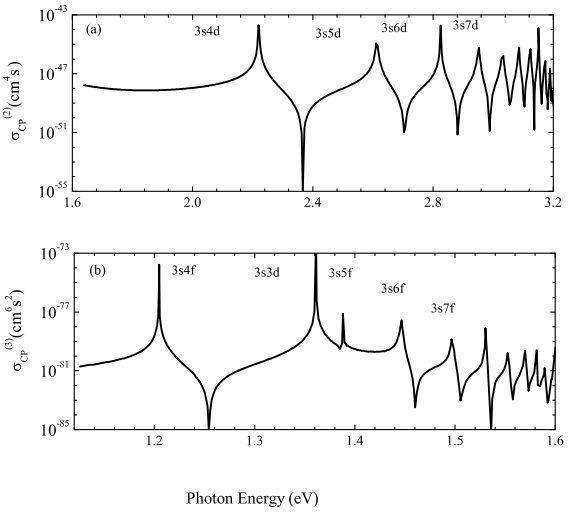

FIG. 4: (a) Two-photon ionization cross section, $\sigma^{(2)}_{CP}$, and (b) three-photon ionization cross section, $\sigma^{(3)}_{CP}$, from the first excited state $3s3p\ ^1P$ by the CP field.

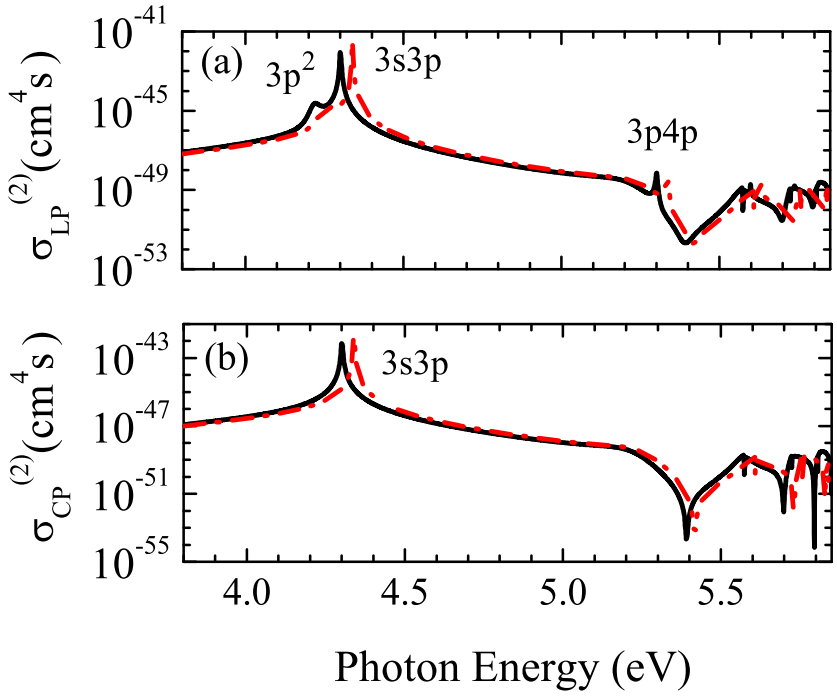

FIG. 5: (Color Online) Comparison of the total two-photon ionization cross sections by the (a) LP field, $\sigma^{(2)}_{LP}$, and (b) CP field, $\sigma^{(2)}_{CP}$, as a function of photon energy using the FCHFP (solid) and MP^b (dot-dashed).

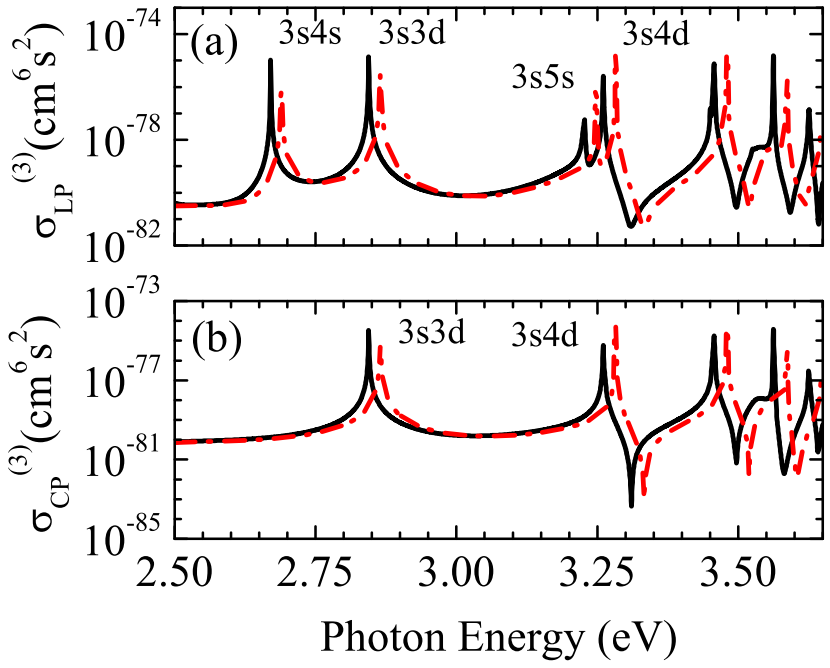

FIG. 6: (Color Online) Same as those in Figs. 5(a) and (b) but for three-photon ionization.

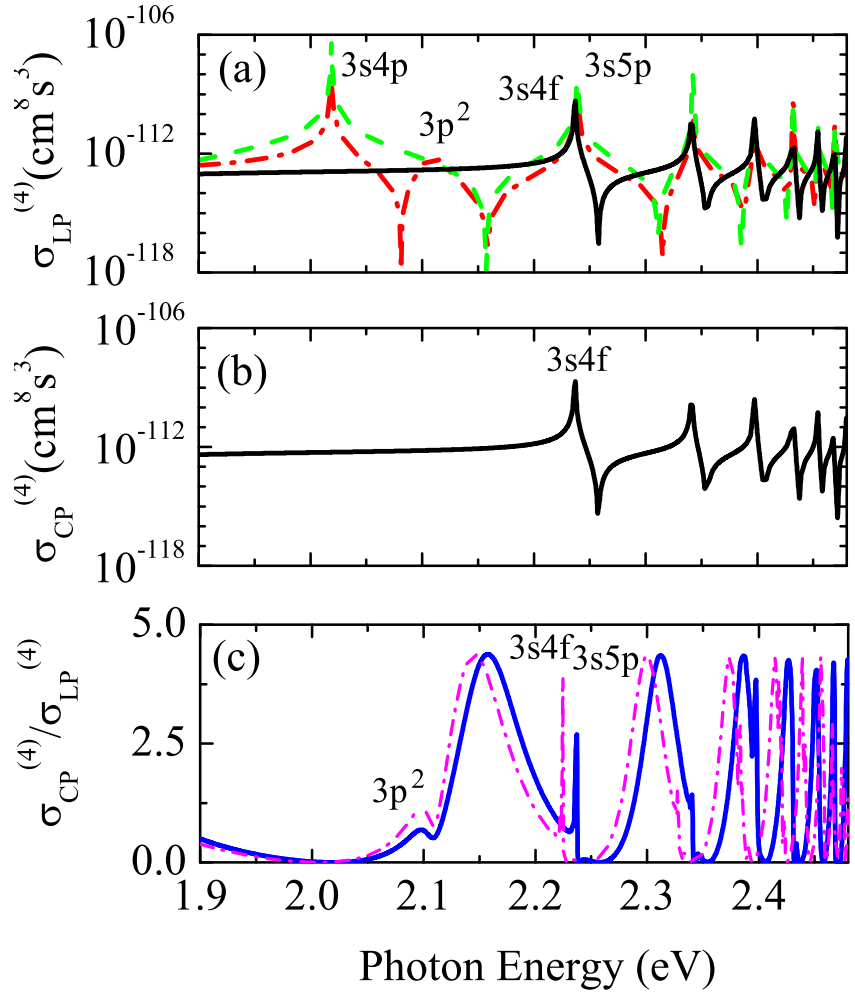

FIG. 7: (Color Online) Same as those in Figs. 5(a) and (b) but for four-photon ionization.